frontiers | Frontiers in Earth Science

TYPE Original Research
PUBLISHED 11 August 2023
DOI 10.3389/feart.2023.1141263

OPEN ACCESS

EDITED BY
Ying Wu,
East China Normal University, China

REVIEWED BY
Andre L. Belem,
Fluminense Federal University, Brazil
Franck Bassinot,
UMR8212 Laboratoire des Sciences du Climat et de l'Environnement (LSCE), France

*CORRESPONDENCE
Maria Caezare Mae R. Cariño,
mrcarino2@up.edu.ph

RECEIVED 10 January 2023
ACCEPTED 10 July 2023
PUBLISHED 11 August 2023

CITATION
Cariño MCMR, Peleo-Alampay AM, Wiesner MG, de Silva LP, Lahajnar N, Betzler C, Fikree I and Lüdmann T (2023), Planktonic foraminifera fluxes and their response to the Asian Monsoon: insights from the Maldives, Indian Ocean. *Front. Earth Sci.* 11:1141263. doi: 10.3389/feart.2023.1141263

Planktonic foraminifera fluxes and their response to the Asian Monsoon: insights from the Maldives, Indian Ocean

Maria Caezare Mae R. Cariño[1]*, Alyssa M. Peleo-Alampay[1], Martin G. Wiesner[1,2], Leopoldo P. de Silva[1], Niko Lahajnar[3], Christian Betzler[3], Ibrahim Fikree[4] and Thomas Lüdmann[3]

[1]Nannoworks Laboratory, National Institute of Geological Sciences, University of the Philippines, Diliman, Philippines, [2]Second Institute of Oceanography, Hangzhou, China, [3]Institute of Geology, Universität Hamburg, Hamburg, Germany, [4]Environment and Monitoring Section, Ministry of Tourism, Male, Maldives

This study describes seasonal changes in the fluxes of planktonic foraminifera in response to changes in environmental conditions during the Asian Monsoon. Sediment trap systems were deployed for a period of 1 year at two locations in the Maldives: Kardiva Channel and Inner Sea. Twenty-six (26) planktonic foraminifera were recognized, of which six species (*Trilobatus sacculifer*, *Globorotalia menardii*, *Globigerinoides ruber*, *Globigerina siphonifera*, *Neogloboquadrina dutertrei*, and *G. bulloides*) dominated the assemblage (82%–84%) in both sites. Planktonic foraminifera fluxes and chlorophyll-a concentrations are higher in the Inner Sea. Total planktonic foraminifera fluxes show preference to high nutrient conditions during monsoon periods. Planktonic foraminifera fluxes generally follow the trend of carbonate fluxes except during October-November 2014. Species flux generally reached maximum during the NE monsoon as a response to increase in nutrient concentration brought by the movement of the North Equatorial Current over the trap sites. The expansion of nutrient-rich surface waters, occurring eastward during the SW monsoon and westward during the NE monsoon, led to an increase in the population of species dwelling in both shallow (*T. sacculifer* and *G. ruber*) and deep waters (*N. dutertrei* and *G. bulloides*). Dominance of shallow-dwelling species *T. sacculifer* and *G. ruber* throughout the sampling period suggests stable stratification of the water column. This supports the idea of wind-mixing rather than local upwelling as the driving force for enrichment of nutrients and subsequent increase in planktonic foraminifera fluxes. Lateral advection and resuspension in settling of particles to the traps is evident based on the presence of benthic foraminifera in the Inner Sea samples. These processes, however, did not significantly mask climate and surface ocean signals since there remains a clear correlation between planktonic foraminifera fluxes and environmental conditions.

KEYWORDS

Asian monsoon, planktonic foraminifera, sediment trap fluxes, Maldives, Indian Ocean

1 Introduction

Planktonic foraminifera are important indicators of environmental changes in modern oceans. Plankton tows and surface sediments provide data on the occurrence and distribution of modern planktonic foraminifera in the Indian Ocean (e.g., Bé and Hutson, 1977; Duplessy et al., 1981; Chowdhury et al., 2003; Bhadra and Saraswat, 2021; Shen et al., 2023). Sediment cores on the other hand allow the use of planktonic foraminifera in reconstructing past Indian Ocean surface conditions (e.g., Ahmad et al., 2008; Tantawy et al., 2009; Raza and Ahmad, 2013; Tang et al., 2021; Wang et al., 2021). In recent years, sediment trap studies in the Indian Ocean have been used not only to document seasonal distribution of planktonic foraminifera but also to understand the relationship between surface occurrence and what is delivered and preserved in the sediments (e.g., Curry et al., 1992; Guptha et al., 1997; Conan and Brummer, 2000; Schulz et al., 2002; Ramaswamy and Gaye, 2006). Sediment traps act as effective tools for integrating temporal information regarding the accumulation of planktonic foraminifera tests that settle to the surface of the ocean (e.g., Chaabane et al., 2023).

Seasonal variation of planktonic foraminifera has been studied in the northern Indian Ocean. In the Arabian Sea, increase in planktonic foraminifera flux has been related to upwelling events. During peak SW monsoon, production of planktonic foraminifera increases with dominance of *Globigerina bulloides* (Curry et al., 1992). Schulz and others (2002) reported an increase in flux of planktonic foraminifera during the NE monsoon associated with an upwelling event in the western side of the basin. Similar trend is observed in the Bay of Bengal where planktonic foraminifera are prominent contributors to flux and were observed to increase coinciding with the monsoons (Guptha et al., 1997).

The Maldives is a North-South trending archipelago located in the North equatorial Indian Ocean. It is composed of 26 atolls arranged in two rows enclosing an inner basin, the Inner Sea (Figure 1). The widest passage connecting the Inner Sea with the surrounding ocean is the Kardiva Channel. Studies on planktonic foraminifera species diversity in Maldives sediments described changes in sedimentation of atolls during the Holocene (e.g., Parker and Gischler, 2011; Storz et al., 2014; Tang et al., 2021). However, there are no known published sediment trap studies in the Maldives that focus on planktonic foraminifera fluxes. In this study, we analyze the response of planktonic foraminifera to hydrographic changes during the monsoon period using a 1-year deployment of sediment traps in the Kardiva Channel and in the southern part of the Inner Sea. In addition, Betzler and others (2017) consider the Maldives Inner Sea as a natural sediment trap which preserves a 25 Myrs record of paleoenvironmental changes in the Indian Ocean. Understanding the modern-day behavior of planktonic foraminifera in relation to productivity and circulation is important in paleoceanographic reconstruction based on sediment cores.

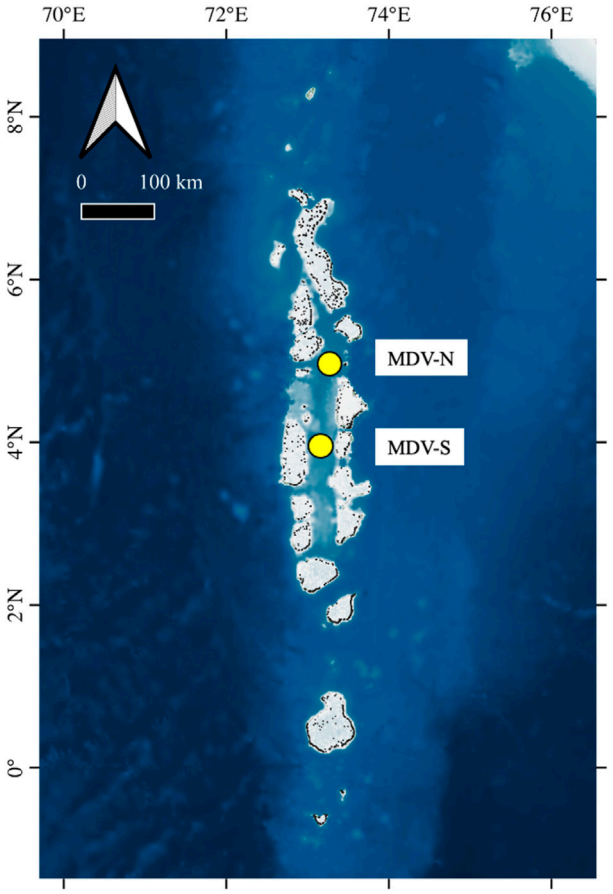

FIGURE 1
Location of mooring arrays in the Maldives. Topographic and bathymetric data are from GEBCO (2022) and Global Administrative Areas (2022).

1.1 Oceanographic setting

The Northern Indian Ocean is highly influenced by the reversing wind directions of the monsoons (Figures 2A, B). Northeasterly winds of the Winter Monsoon are relatively weak (4.9 ms^{-1}; Kench and Brander, 2006) and bring dry air to Southern Asia. The reversed pressure gradient during the Summer Monsoon results to strong southwesterly winds (5.1 ms^{-1}; Kench and Brander, 2006). The strong winds trigger upwelling of nutrient-rich waters and transport of lithogenic material from deserts of Arabia and Somalia (Clemens et al., 1991).

Seasonally reversing winds over the Indian Ocean affect the upper water circulation flow between the Arabian Sea and Bay of Bengal (Figures 2A, B). During the Winter Monsoon, the East India Coastal Current (EICC) flows along the coast to the West, meeting the well-established Northeast Monsoon Current (NMC). Extensions of the NMC flow into the Bay of Bengal and feed the West India Coastal Current (WICC). The Summer Monsoon is characterized by a generally anticyclonic wind pattern and stronger winds than the Winter Monsoon (Beal et al., 2013). The WICC flows southward and feeds the Southwest Monsoon Current (SMC). The SMC flows northward into the Bay of Bengal and supplies water to the East India Coast Current (EICC).

The Maldives lie in the tropics and in the range of the South Asian Monsoon (Kottek et al., 2006; Storz and Gischler, 2011). The number of inter-atoll channels correlates with the intensity of the monsoon and decreases in southern direction (Gischler et al., 2013).

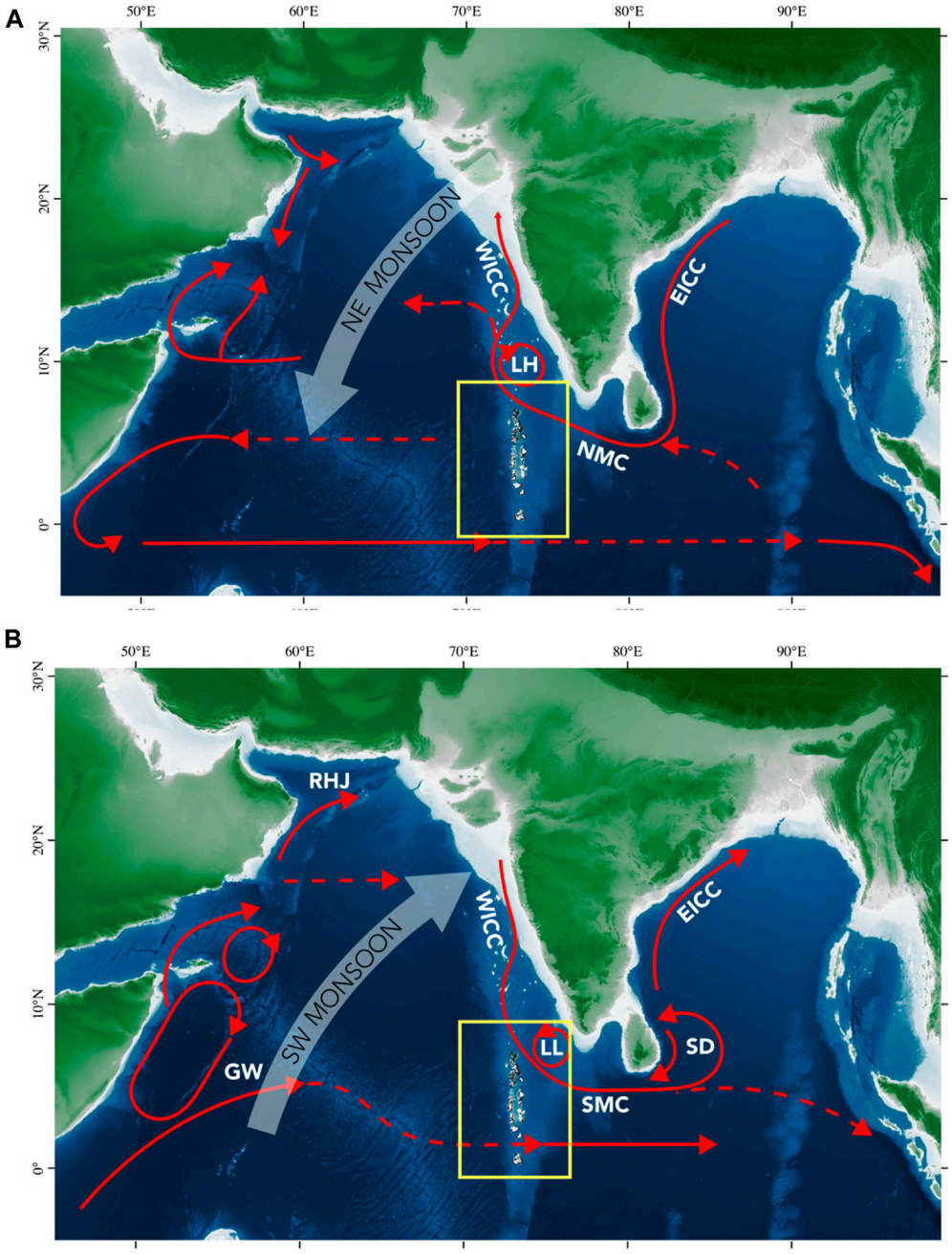

FIGURE 2
Flow of currents during the **(A)** NE monsoon and **(B)** SW monsoon. Current branches indicated are the South Equatorial Counter Current (SECC), Great Whirl (GW), Ras al Hadd Jet (RHJ), Sri Lanka Dome (SD), West Indian Coast Current (WICC), East Indian Coast Current (EICC), Laccadive High and Low (LH and LL), Southwest and Northeast Monsoon Current (SMC and NMC). Surface water circulation in the Northern Indian Ocean was redrawn from Schott and McCreary (2001). Topographic and bathymetric data are from GEBCO (2022) and Global Administrative Areas (2022).

In the passages of the atolls the currents reach velocities up to 2 ms^{-1} (Preu and Engelbrecht, 1991; Owen et al., 2011). Acoustic Doppler Current Profiler (ADCP) and CTD measurements in the Inner Sea during winter and summer monsoon season show a partitioning of the water column into two water masses (Lüdmann et al., 2013; 2018; 2022a; Reolid et al., 2017). A wind-driven mixed layer prevails down to ca. 100 m, followed by a water mass that reaches down to the basin floor. Average temperatures in the surface mixed layer varied between 28°C and 29°C and salinity attains values of around 35.8. The lower layer is characterized by a temperature of 10°C–15°C and a salinity of 35.4, corresponding to the physical properties of the Indian Equatorial Water (Emery, 2019). ADCP measurements in the Inner Sea, executed during winter monsoon season reveal that the upper water mass is directly driven by the monsoon wind and deflected to the southwest. The lower water mass, however, shows a northward flow in the Inner Sea (Lüdmann et al., 2013).

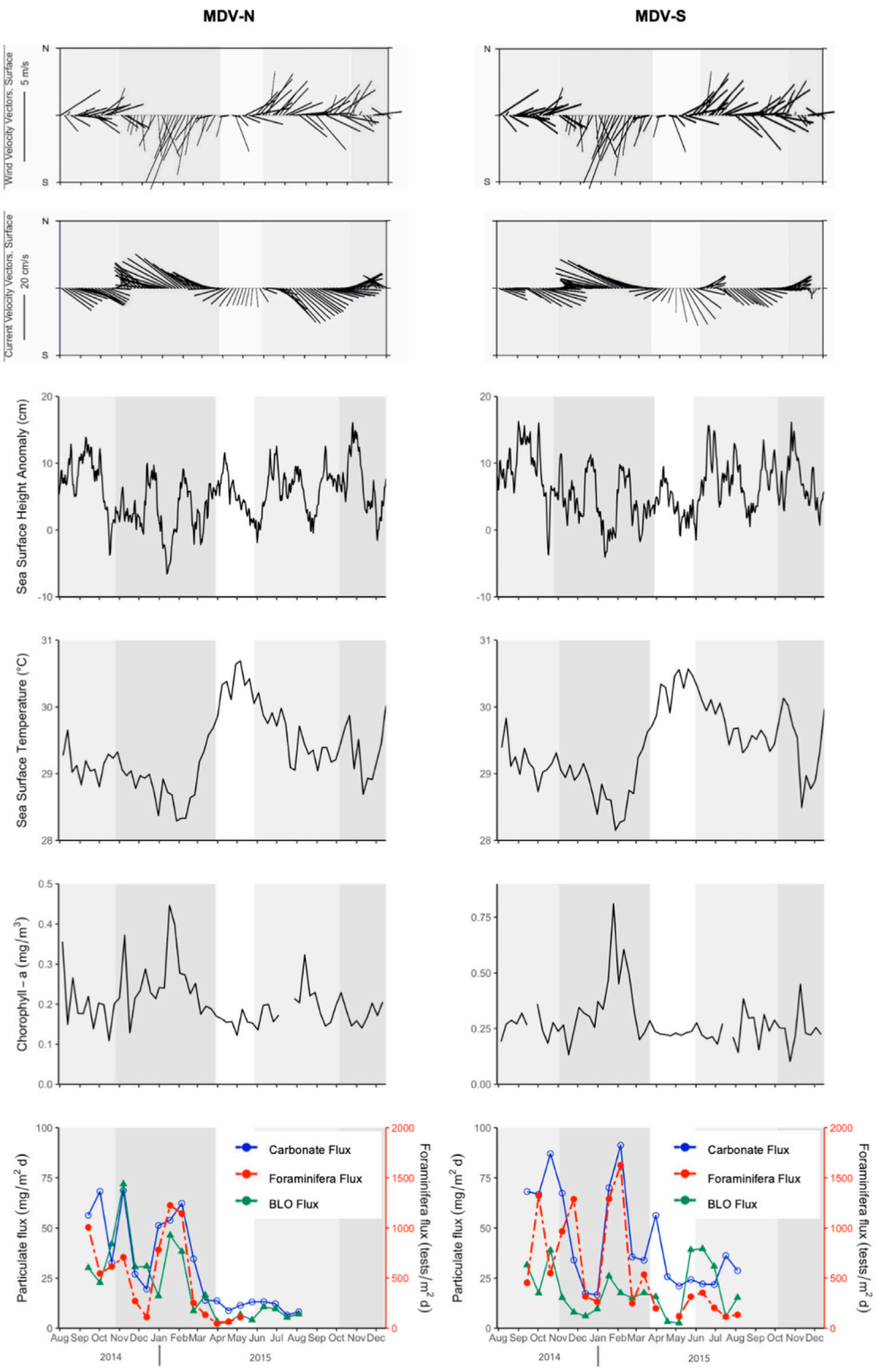

FIGURE 3
Time-series of wind and current velocities, sea surface height anomalies, sea surface temperature, chlorophyll-a, and the fluxes of carbonate, planktonic foraminifera and the sum of biogenic opal, lithics and organic matter (BLO) flux at Sites MDV-N and MDV-S. Dark gray shading corresponds to the NE monsoon, light gray for the SW monsoon periods.

Astronomical tides are in the range of 40–100 cm causing a bidirectional current flow within the large inter-atoll gateways and smaller intra-atoll channels.

2 Materials and methods

2.1 Sediment trap sampling

Two sediment trap mooring systems were deployed during R/V Sonne Cruise SO-236 at 4°55.91′N, 73°17.01′E (MDV-N; total water depth 534 m) in the Kardiva Channel and at 3°55.26′N, 73°08.34′E (MDV-S; total water depth 380 m) in the southern part of the Inner Sea (Figure 3). A shallow sediment trap (Kiel K/MT 234) located at 78 m and a deeper trap (McLane Mark 7G-21) at 200 m below the surface were deployed at Site MDV-N while one trap (McLane Mark 7G-21) at 195 m below the surface was deployed at Site MDV-S. Each trap was programmed to collect sinking particles from 27 August 2014 to 04 August 2015 at intervals of 18 days. However, the shallow sediment trap at Site MDV-N was overgrown with gorgonian corals and could not be utilized for this study. Sediment traps facilitate an understanding of plankton dynamics in the upper water column all year round. It has to be kept in mind, however, that there are uncertainties related to the use of these tools, such as trapping efficiency that might compromise the validity of the results (Butman, 1986; Buesseler et al., 2007). Nonetheless, they are an appropriate tool for gaining insights in vertical particle flux patterns.

Prior to deployment, the sample bottles were filled with sea water from the respective trap depths. The water was filtered through WHATMAN GF/F filters (precombusted at 450°C) and analytical grade sodium chloride (35 g NaCl l^{-1}) and mercury chloride (3.3 g $HgCl_2$ l^{-1}) were added in order to minimize diffusive processes and retard microbial activity in the trapped material. After recovery, the wet samples were passed through a 1-mm mesh nylon sieve to exclude zooplankton that had been able to swim through the trap entrance baffle into the sample bottles. These 'swimmers' (mainly pteropods, and some copepods) on the 1 mm sieve were gently washed with a small volume of filtered seawater to dislodge any <1 mm material entrapped on the sieve; smaller copepods were picked with forceps from the <1 mm fraction. Subsequently the <1 mm fractions were split into aliquots by a high-precision KUM-splitter, then filtered on pre-weighed Nuclepore filters (0.45 µm pore size) and dried at 40°C for 72 h. The dry weights of these fractions were used to calculate major component (carbonate, organic matter biogenic opal and lithogenics) and foraminifera species analyses. Major component analyses were performed according to the procedures given in Ran et al. (2015).

2.2 Foraminifera analysis

A total of 32 samples were used in this study. Due to low sediment recovery, samples from five MDV-N cups (May—August 2015) from and one MDV-S cup (April 2015) were insufficient for foraminifera studies. Aliquots were removed from the filters, diluted with buffered distilled water (pH = 9) and ultrasonicated for 1 min to disaggregate the particles. Subsequently, the suspension was wet-sieved through 125 and 63 µm stainless steel sieves for separation of juvenile and mature foraminifera. The >63 µm fraction was oven dried (at 60°C) for 24 h. Foraminifera specimens were picked from the >63 µm fraction using a very fine brush viewed under an Olympus binocular microscope (×45 magnification). Specimens were separated and mounted to slides coated with gum tragacanth. Identification of foraminifera was based on descriptions in mikrotax (Young et al., 2017) and Saito and others (1981). Planktonic foraminifera fluxes (specimens/m^2day) were calculated using number of specimens, split fraction, length of collection time (18 days), and opening area of the trap cone (0.5 m^2).

2.3 Remote sensing data

Weekly surface wind speeds were downloaded from the National Centers for Environmental Prediction (NCEP)/National Center for Atmospheric Research (NCAR) Reanalysis Project 1 with a spatial resolution of 1/4° × 1/4° (National Oceanic and Atmospheric Administration, 2023). Surface current velocity vectors were taken from the Ocean Surface Current Analyses Real-Time (OSCAR) data sets (National Oceanic and Atmospheric Administration, 2022) with a spatial resolution of 1/3° and temporal resolution of 5 days. Weekly sea surface temperatures of 0.25° × 0.25° resolution were acquired from the NCEP Climate Modeling Branch (CMB) (National Oceanic and Atmospheric Administration, 2015). 8-day chlorophyll-a (CHL) concentrations (MODIS-Aqua, 4-km resolution) were downloaded from GES-DISC Interactive Online Visualization and analysis Infrastructure (National Aeronautics and Space Administration, 2022) and taken as a metric for productivity. Sea surface height anomalies were calculated from 10-year mean daily sea surface heights from Copernicus (Copernicus, 2020).

3 Results and discussion

3.1 Carbonate fluxes

Carbonate fluxes in the North trap range from 6.56 mg $m^{-2}d^{-1}$–68.70 mg $m^{-2}d^{-1}$ with an average of 30.28 mg $m^{-2}d^{-1}$. Three distinct peaks were observed. First was during the SW monsoon and two peaks during the NE monsoon corresponding to increase in chlorophyll-a concentration and low SST values. In the South trap, similar peaks are observed. Here, carbonate fluxes range from 16.64 mg $m^{-2}d^{-1}$–91.23 mg $m^{-2}d^{-1}$ with an average of 43.39 mg $m^{-2}d^{-1}$. High fluxes were seen during the SW and NE monsoons. Flux maxima were recorded during the NE monsoon associated with highest chlorophyll-a concentration and lowest SST.

3.2 Monsoonal forcing

Planktonic foraminifera (pforam) fluxes generally respond to changes in oceanographic conditions brought by seasonally reversing monsoons. Changes in strengths of cyclonic and

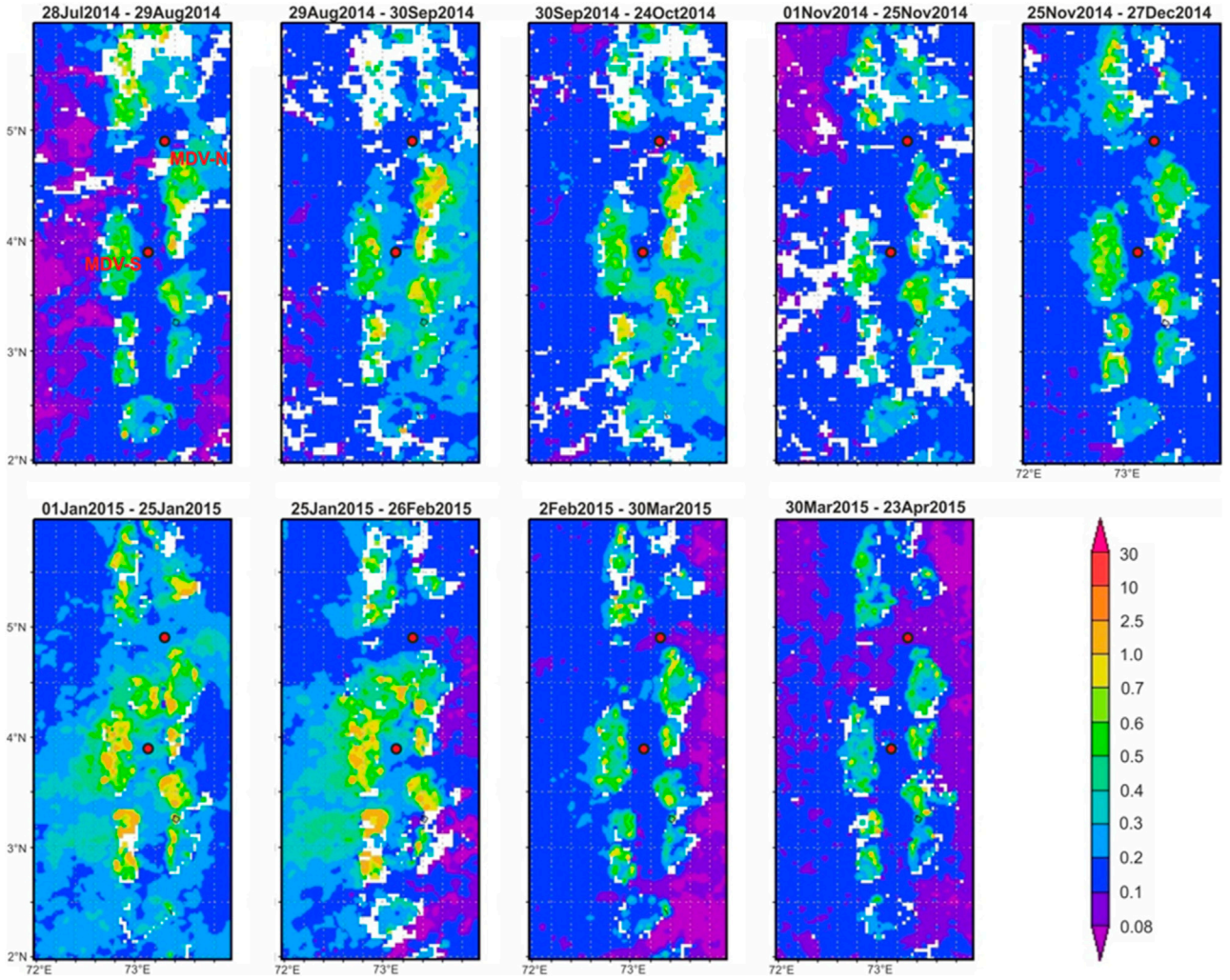

FIGURE 4
Maps of chlorophyll-a concentration from July 2014—April 2015 in the Maldives.

anticyclonic eddies that pass through the Kardiva Channel and Inner Sea are observed throughout the sampling period. Chlorophyll-a concentrations in the South trap (MDV-S) are relatively higher than in the North trap (MDV-N). The 2014 SW monsoon is largely subjected to the movement of anticyclonic eddies (Site MDV-N average Sea Surface Height Anomalies (SSHA): +7.5 cm; Site MDV-S average SSHA: +8.9 cm). This is coupled with an increase in chlorophyll-a concentration and low SST (Figures 3, 4). Anticyclonic eddies also control circulation during the NE monsoon with an exception during January 2015 when cyclonic eddies are a major contributor (Site MDV-N average SSHA: −2.4 cm; Site MDV-S average SSHA: −1 cm). Surface water cooling is related to wind mixing as the North Equatorial Current moves across the trap sites (Sasamal, 2006; 2007). This wind mixing creates a rise in chlorophyll-a concentration as it pumps nutrient-rich waters from deeper waters to the surface (Figures 3, 4). The intermonsoon period and 2015 SW monsoon are characterized by low productivity and marked by low wind speeds and high SST. Together with high precipitation in 2015 (Chaudhuri et al., 2021), these conditions generally inhibit the production of biogenic materials (Unger et al., 2003).

3.3 Total planktonic foraminifera flux

The pforam fluxes in both traps display strong seasonal patterns with three distinct peaks (Figure 3). The first of the three peaks was observed during the SW monsoon. Pforam fluxes are lower at Site MDV-N (1,006 tests $m^{-2}day^{-1}$) compared to Site MDV-S (1,323 tests $m^{-2}day^{-1}$). Two peaks during the NE monsoon occur during the start (November 2014) and mid-monsoon (January-February 2015). Pforam fluxes in the northern trap during these times are 709 tests $m^{-2}day^{-1}$ and 1,225 tests $m^{-2}day^{-1}$. While in the southern trap, peak pforam fluxes during the NE monsoon are 1,287 tests $m^{-2}day^{-1}$ and 1,626 tests $m^{-2}day^{-1}$. Pforam fluxes generally follow the trend of carbonate fluxes except during October-November 2014 when there is an increase in BLO (biogenic opal, lithics, and organic matter) fluxes (Figure 3). During this period, calcareous nannofossil flux

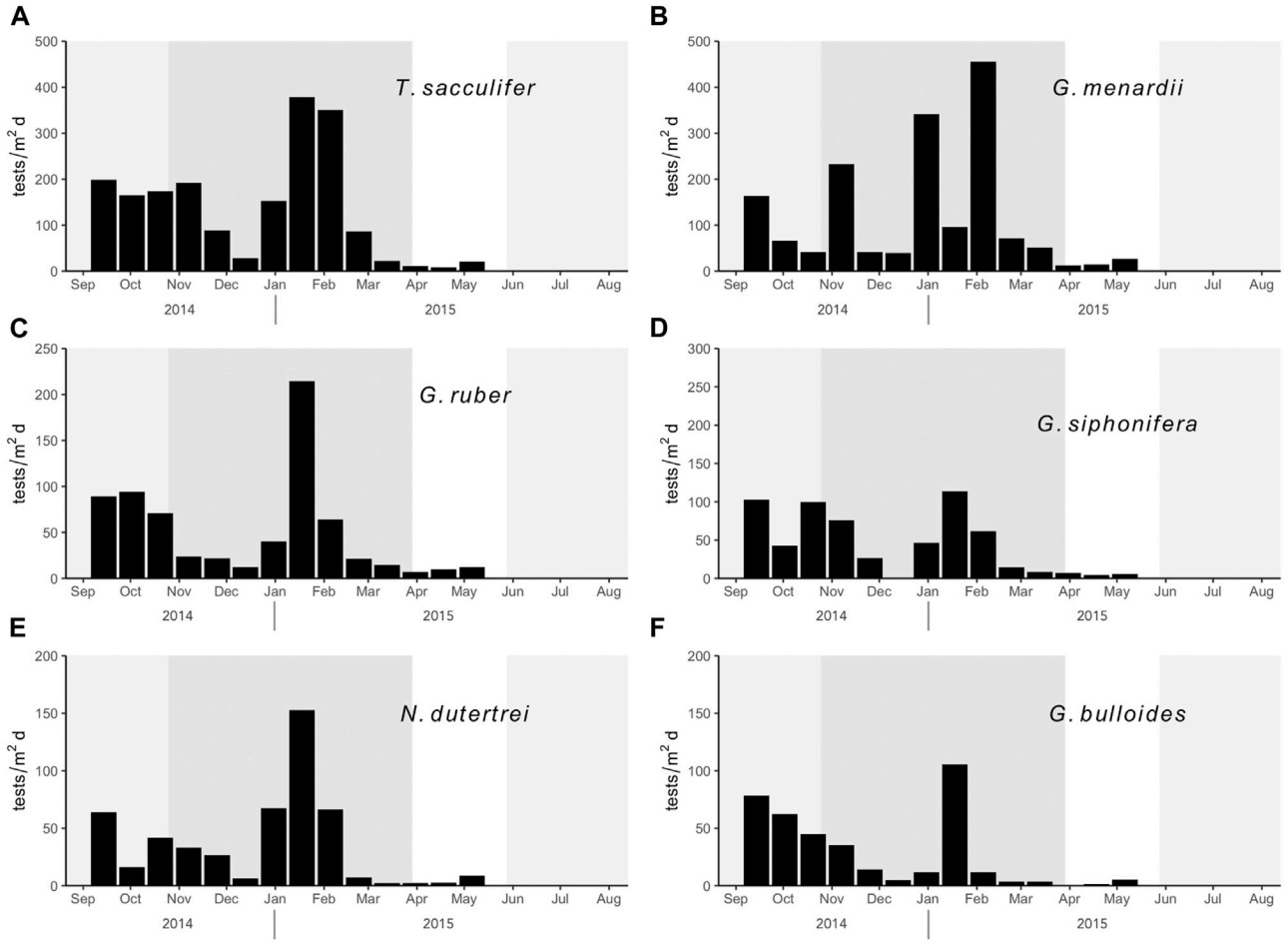

FIGURE 5
Comparison of the fluxes of the six most abundant planktonic foraminifera species at Site MDV-N. **(A)** *Trilobatus sacculifer* **(B)** *Globorotalia menardii* **(C)** *Globigerinoides ruber* **(D)** *Globigerina siphonifera* **(E)** *Neogloboquadrina dutertrei* **(F)** *Globigerina bulloides*.

significantly increased taking over bulk of the carbonate flux (Cariño, unpublished data). A sudden decrease in pforam fluxes during the 2014 SW monsoon (October-November) in the South trap may indicate the contribution of other carbonate organisms to the total carbonate flux.

3.4 Seasonality of individual planktonic foraminifera species

A total of 26 foraminifera species were identified. Six species show seasonal flux patterns and contributed to 82% and 84% of the total assemblage at Sites MDV-N and MDV-S, respectively. These are *Trilobatus sacculifer*, *Globorotalia menardii*, *Globigerinoides ruber*, *Globigerina siphonifera*, *Neogloboquadrina dutertrei*, and *Globigerina bulloides* (Figures 5, 6).

3.4.1 Trilobatus sacculifer

Trilobatus sacculifer is the most abundant species in the sampling area. It accounts for 27% of total foraminifera counts in the northern trap and 24% in the southern trap. *T. sacculifer* is characterized by a well-defined seasonal flux pattern where it exhibits peaks in the SW and NE monsoon. A distinct peak in January to February in both traps was observed. Flux ranges from 22 to 378 tests m^{-2} day^{-1} in the North trap and 57–455 tests m^{-2} day^{-1} in the South trap during this time. The intermonsoon and 2015 SW monsoon flux rates of *T. sacculifer* do not exceed 92 tests m^{-2} day^{-1} in both traps.

T. sacculifer is generally considered as a common species of the tropical region (Schiebel and Hemleben, 2001). *T. sacculifer* is spinose and often bearing symbiotic algae making them typical inhabitants of the photic zone (Hemleben et al., 1989). Previous sediment trap studies observe *T. sacculifer* during high nutrient events associated with the monsoons. In the western Arabian Sea, *T. sacculifer* showed increase in production associated with wind mixing off Somalia during January and February (Conan and Brummer, 2000) and immediately after the onset of SW monsoon upwelling (Curry et al., 1992).

3.4.2 Globorotalia menardii

Globorotalia menardii is the second most abundant species observed in both traps accounting for 23% of total assemblages in the North trap and 21% in the South trap. It is observed on both sampling traps to exhibit multiple peaks during the SW and NE

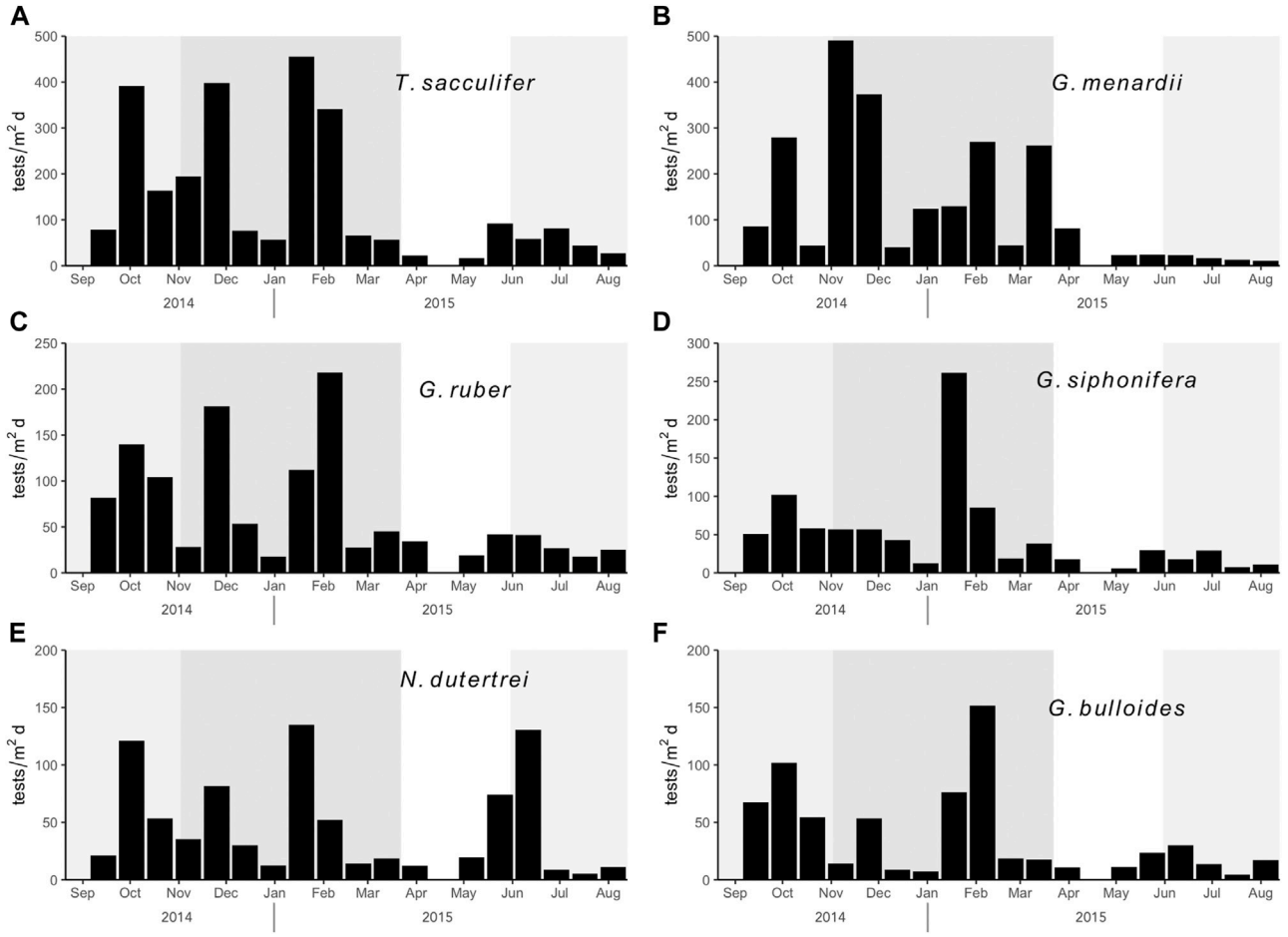

FIGURE 6
Comparison of the fluxes of the six most abundant planktonic foraminifera species at Site MDV-S. **(A)** *Trilobatus sacculifer* **(B)** *Globorotalia menardii* **(C)** *Globigerinoides ruber* **(D)** *Globigerina siphonifera* **(E)** *Neogloboquadrina dutertrei* **(F)** *Globigerina bulloides*.

monsoons. Like *T. sacculifer*, an increase in *G. menardii* flux was observed during January-February. This peak is more prominent in the North trap where it recorded the maximum flux during February (455 tests m^{-2} day^{-1}). In the South trap, fluxes range from 11 to 491 tests m^{-2} day^{-1} with peak flux around November. A sharp decrease in flux toward the end of NE monsoon in both traps extend to the SW monsoon.

G. menardii is described to be a dominant species of the subtropical—tropical Indian Ocean (Bé and Hutson, 1977). *G. menardii* is non-spinose and consume phytoplankton which they sometimes keep as symbionts (Hemleben et al., 1989). At the trap sites, *G. menardii* shows an erratic trend, increasing and decreasing multiple times during monsoon periods. This supports previous studies that *G. menardii* can sometimes change its habitat from deep to shallow waters (Thunnel and Reynolds, 1984; Hemleben et al., 1989).

3.4.3 Globigerinoides ruber

G. ruber showed maximum flux in both traps during the NE monsoon (around January). In the North trap, fluxes ranged from 7 tests m^{-2} day^{-1} to 214 tests m^{-2} day^{-1} with an average flux of 50 tests m^{-2} day^{-1}. While in the South trap, fluxes ranged from 17 tests m^{-2} day^{-1} to 218 tests m^{-2} day^{-1} with an average flux of 67 tests m^{-2} day^{-1}. Low fluxes are recorded during the intermonsoon and 2015 SW monsoon in both traps.

Like *T. sacculifer*, *G. ruber* is a spinose shallow-dwelling species with dinoflagellates as symbionts (Hemleben et al., 1989). *G. ruber* is commonly observed in tropical—subtropical waters during periods of warm stratified waters (Sautter and Thunnel, 1991). Yamasaki and Oda (2003) demonstrated the affinity of *G. ruber* to high SST in the Okinawa Trough during autumn. During this time, the passing Kuroshio Current brings warm water consequently mixing surface waters and deepening thermocline. This is supported by a study by Xu et al. (2005) in Ryukyu Islands where *G. ruber* was reported to flourish in well stratified and high surface temperatures during autumn, spring, and summer. However, in the Panama Basin, maximum flux of *G. ruber* was observed during upwelling event of February-March and not during the warming of surface waters in August (Thunell and Reynolds, 1984).

3.4.4 Globigerina siphonifera

Species flux of *G. siphonifera* in the North trap range from 6 tests m^{-2} day^{-1} to tests m^{-2} day^{-1} with an average flux of 47 tests m^{-2} day^{-1}. In the South trap, *G. siphonifera* flux ranged from 6 tests m^{-2} day^{-1} to 261 tests m^{-2} day^{-1} with average flux of 49 tests m^{-2} day^{-1}. Flux patterns of *G. siphonifera* in the South trap show maximum during January to February (261 tests m^{-2} day^{-1}) where it recorded twenty-two times increase from the previous sampling interval. Other sampling cups did not record *G. siphonifera* flux greater than 101 tests m^{-2} day^{-1}.

G. siphonifera is spinose and possesses symbionts (Hemleben et al., 1989). Sediment trap flux studies of *G. siphonifera* revealed its strong correlation with the monsoons. Highest fluxes were seen in February—March in the Panama Basin corresponding to records of high productivity (Thunnel and Reynolds, 1984). In the Bay of Bengal, species flux of *G. siphonifera* showed prominent increase during the monsoon periods but with greatest flux during the SW monsoon upwelling period (Guptha et al., 1997). *G. siphonifera* was also observed to increase in flux during the NE monsoon upwelling in the Somalia Basin during January to February (Conan and Brummer, 2000).

3.4.5 Neogloboquadrina dutertrei

N. dutertrei fluxes in the North trap range from 2 tests m^{-2} day^{-1} to 153 tests m^{-2} day^{-1} with an average flux of 35 tests m^{-2} day^{-1}. In the South trap, flux ranged from 5 tests m^{-2} day^{-1} to 123 tests m^{-2} day^{-1} with an average flux of 46 tests m^{-2} day^{-1}. Maximum fluxes for both traps were recorded during the NE monsoon.

N. dutertrei is a non-spinose species commonly found in tropical waters (Hemleben et al., 1989). Studies on the seasonality of *N. dutertrei* showed its preference to upwelling conditions (Guptha et al., 1997; Conan and Brummer, 2000) and thermocline movement (Thunell and Reynolds, 1984). In the Panama Basin, high flux of *N. dutertrei* were attributed to intense upwelling causing an increase in primary productivity and shallowing of thermocline (Thunell and Reynolds, 1984). In the San Pedro Basin, increase in *N. dutertrei* flux occurred immediately after upwelling and marked the stabilization and eventual stratification of the water column (Sautter and Thunell, 1991). Yamasaki and Oda (2003) showed the abundance of *N. dutertrei* flux in the Okinawa Trough which was associated with upwelling and shoaling of thermocline in January—February.

3.4.6 Globigerina bulloides

Species flux of *G. bulloides* in the North trap reach up to 105 tests m^{-2} day^{-1} with an average flux of 27 tests m^{-2} day^{-1}. While in the South trap, fluxes range from 4 tests m^{-2} day^{-1} to 152 tests m^{-2} day^{-1} with an average flux of 38 tests m^{-2} day^{-1}. Maximum fluxes in both traps were observed during the NE.

G. bulloides is a spinose species and does not bear any symbionts (Hemleben et al., 1989). Like *N. dutertrei*, *G. bulloides* is a deep-dwelling species (above the thermocline) and is widely used an upwelling indicator in transitional to polar waters (Hemleben et al., 1989). High fluxes were recorded in the Panama Basin during the summer with minor increase during February—March (Thunell and Reynolds, 1984). In the San Pedro Basin, *G. bulloides* peak fluxes were related to heightened food availability during winter and intense upwelling (Sautter and Thunell, 1991). Sediment trap studies in the Arabian Sea and Bay of Bengal record highest fluxes of *G. bulloides* during the SW monsoon related to upwelling events (Curry et al., 1992; Guptha et al., 1997; Conan and Brummer, 2000).

3.5 Shallow vs. deep dwelling species

The six most abundant species can be divided into groups depending on their vertical distribution in the water column. The first group are shallow dwelling species characterized as spinose and bearing algal symbionts (Hemleben et al., 1989). They are composed of *T. sacculifer, G. ruber* and *G. siphonifera*. These species are commonly observed during months of warm SST. Deep dwelling species on the other hand are non-spinose and may bear symbionts facultatively (Hemleben et al., 1989). These include *G. menardii, N. dutertrei,* and *G. bulloides*. Their abundance in trap samples indicate enrichment of cold nutrient rich waters to the surface during upwelling events (e.g., Thunnel and Reynolds, 1984; Guptha et al., 1997; Yamasaki and Oda, 2003).

Affinity of species to high nutrient environments can be observed by plotting shallow dwelling (oligotrophic species) *T. sacculifer* and *G. ruber* against deep dwelling (productivity indicators) *N. dutertrei* and *G. bulloides* (Figure 7). Both shallow and deep dwelling species showed increased fluxes during high chlorophyll-a concentrations in both sampling sites. We suspect that the increase in chlorophyll-a concentrations in the sampling sites is not due to local upwelling but is a consequence of surface wind-driven extension of chlorophyll rich waters eastward during the SW monsoon and westward during the NE monsoon (Figure 4). The dominance of shallow-dwelling species *T. sacculifer* and *G. ruber* throughout the sampling period supports the idea of predominance of strong winds as driver for mixing in the upper water column. Lateral advection of these cold, chlorophyll-rich plumes to the trap site may have produced peaks in productivity (and flux) though SSHA does not indicate significant cyclonic eddy activity at the site.

3.6 Source of particles being advected and resuspended in the Inner Sea and Kardiva Channel

Benthic foraminifera are present in both sampling traps and can serve as evidence for lateral advection and resuspension in the Inner Sea and Kardiva Channel (Figure 8). They were identified to belong to the genera *Spiroloculina* and species *S. wrightii* which are common in surface and core sediments in the Maldivian atolls (Parker and Gischler, 2011; Storz et al., 2014). *S. wrightii* is observed at depths of about 300 m in the Timor Sea (Loeblich and Tappan, 1994). Thus, provenance of observed benthic specimens in the Maldives is most likely from deeper sources. Benthic foraminifera are therefore probably advected and transported from the surrounding atolls (e.g., North Male Atoll, South Male Atoll, Ari Atoll) and resuspended from the immediate sea floor (Kardiva Channel: ~500 m; Inner Sea: ~380 m). High abundance of benthic foraminifera tests was recorded during the SW monsoon in the South trap (Figure 8). Lack of sufficient number of samples limits the observation and comparison in the North trap. Possible

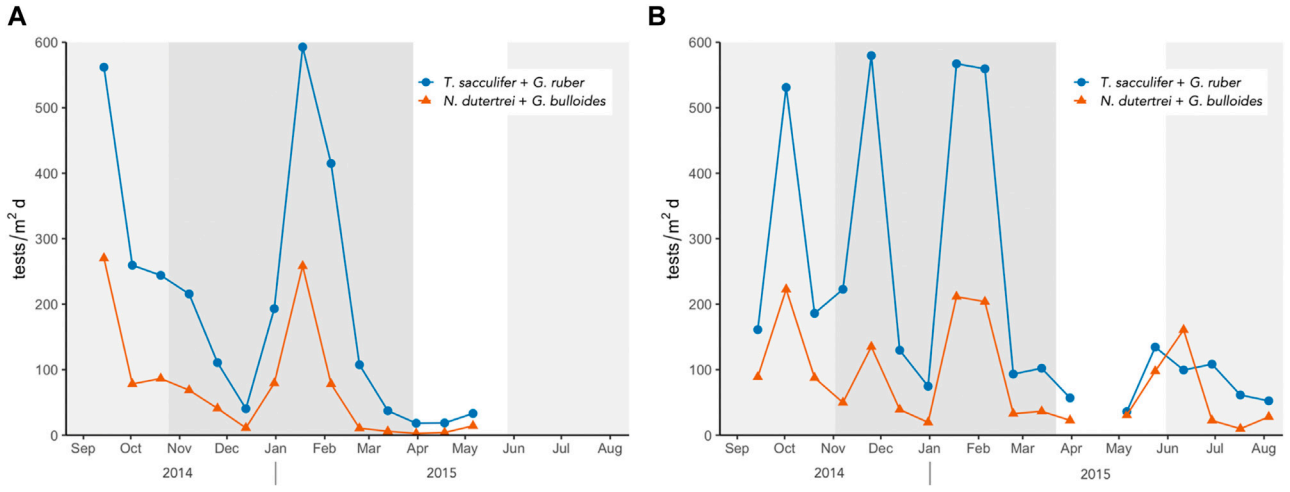

FIGURE 7
Shallow vs. deep dwelling species in **(A)** North trap and **(B)** South trap.

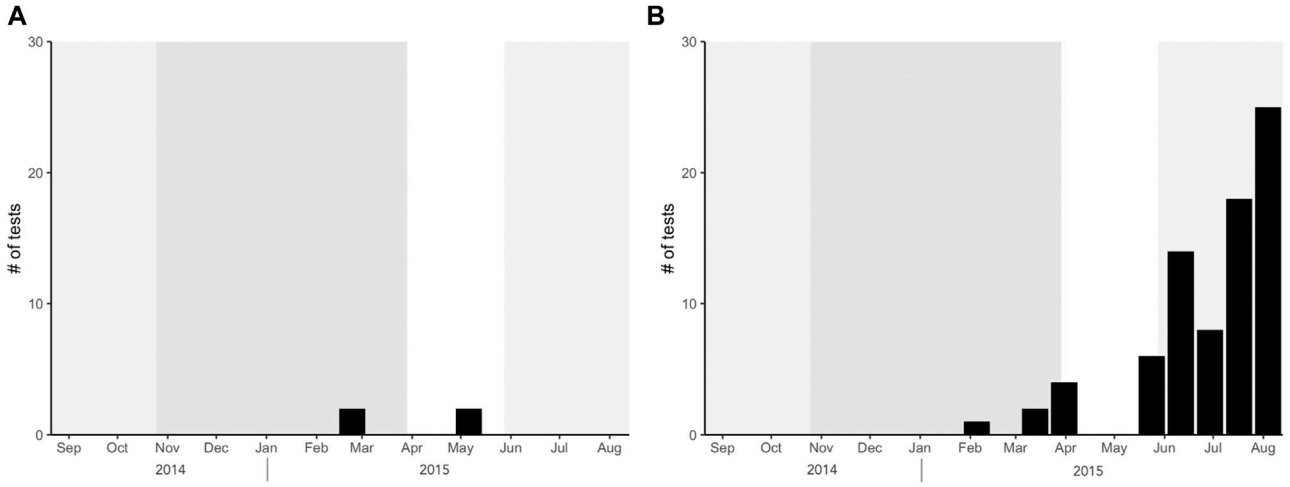

FIGURE 8
Benthic foraminifera abundances in the **(A)** North and **(B)** South traps.

mechanism of transport may include localized submarine landslides in the Inner Sea (e.g., Lüdmann et al., 2022a) and subsequent movement of anticyclonic eddies that lead to local upwelling (northern hemisphere) and transport of benthic foraminifera to the trap sites. The probability of resuspension in the southern trap may also be higher due to the proximity of the trap to the sediment bottom.

The occurrence of benthic foraminifers strongly suggests sediment resuspension and lateral advection in the Inner Sea. Resuspension in the trap area is also indicated by seismic profiles presented by Lüdmann et al. (2022b) which show mass wasting along the steep slopes of the Kardiva Channel. Depending on the sediment erodibility and factors such as current strength and shear stress in the source area it is assumed that resuspension has affected other sediment components such as planktonic tests (and lithics) as well. However, their contribution to the total mass flux can hardly be quantified. Yet, the good correspondence between the planktonic foraminifera fluxes and the environmental conditions revealed by satellite data and *in situ* measurements in the area of sediment traps indicate that resuspended particles did not completely mask climate and surface ocean signals at the sites of particle export. As to sedimentary archives in this area, however, resuspension and lateral advection may lead to significant misinterpretations when the past environmental conditions are extracted from planktonic foraminifera (or diatoms and coccoliths). These reconstructions need to consider that due to lateral advection or resuspension,

biogenic (and lithogenic) sediment fractions may carry information on hydrography and climate not related to the site of investigation.

4 Conclusion

Analysis of 1-year deployment of sediment traps in the Maldives show seasonality of pforam fluxes correlating to the monsoon periods where fluxes tend to exhibit highest fluxes during phases of low SST and high nutrient concentrations. The southern trap exhibited higher pforam fluxes and chlorophyll-a concentrations. A total of 26 species were identified, of which 6 accounted for the majority of total pforam flux. Species assemblage was dominated by sub-tropical to tropical species. Comparison of upwelling and non-upwelling indicators suggests absence of upwelling and dominance of strong winds as main driver for surface water mixing in the Inner Sea of the Maldives. The increased fluxes in both shallow and deep dwelling pforam species are due to the leeward extension of high chlorophyll areas during the monsoons. Benthic foraminifera were identified in the samples which confirms the influence of lateral advection and resuspension in the sinking of sediments into the traps. Good correlation between pforam fluxes and seasonally changing environmental conditions suggests negligible effects of these resuspended particles to climate and surface ocean signals.

Data availability statement

The raw data supporting the conclusion of this article will be made available by the authors, without undue reservation.

Author contributions

MC took the lead as the principal author, being responsible for manuscript preparation. She conducted sample processing for planktonic foraminifera analysis and carried out the flux analysis for this study. AP-A provided guidance to the primary author regarding the structure and flow of the paper. She also collaborated with other authors in data analysis and paper review. MW contributed by providing the samples, which were shipped from Germany to the Philippines. He also shared data on particulate fluxes, satellite observations, and environmental data. MW actively participated in data analysis alongside other authors. LS, as a specialist, examined the trends in planktonic foraminifera fluxes and offered valuable insights during discussions. NL played a crucial role in obtaining the samples through sediment traps during the research expedition. He did the analyses of the major flux components. CB, as the chief scientist of the research cruise, provided valuable suggestions on enhancing the discussion. IF contributed to the conceptualization of the sediment trap study. TL provided relevant information on sediment redistribution in the Inner Sea and contributed graphs illustrating currents. All authors contributed to the article and approved the submitted version.

Funding

Funding from MALSTROM (BMBF Grant 03G0236A) is gratefully acknowledged.

Acknowledgments

The authors would like to express their gratitude to the crew and scientists onboard RV Sonne Cruise SO-236 for the samples used in this study.

Conflict of interest

The authors declare that the research was conducted in the absence of any commercial or financial relationships that could be construed as a potential conflict of interest.

Publisher's note

References

Ahmad, S. M., Babu, G. A., Padmakumari, V. M., and Raza, W. (2008). Surface and deep water changes in the northeast Indian Ocean during the last 60 ka inferred from carbon and oxygen isotopes of planktonic and benthic foraminifera. *Palaeogeogr. Palaeoclimatol. Palaeoecol.* 262, 182–188. doi:10.1016/j.palaeo.2008.03.007

Bé, A. W. H., Hutson, W. H., and Be, A. W. H. (1977). Ecology of planktonic foraminifera and biogeographic patterns of life and fossil assemblages in the Indian Ocean. *Micropaleontology* 22 (4), 369–414. doi:10.2307/1485406

Beal, L. M., Hormann, V., Lumpkin, R., and Foltz, G. R. (2013). The response of the surface circulation of the Arabian Sea to monsoonal forcing. *J. Phys. Oceanogr.* 43, 2008–2022. doi:10.1175/JPO-D-13-033.1

Bhadra, S. R., and Saraswat, R. (2021). Assessing the effect of riverine discharge on planktic foraminifera: A case study from the marginal marine regions of the Western Bay of bengal. *Deep-Sea Res. II* 183, 104927. doi:10.1016/j.dsr2.2021.104927

Buesseler, K. O., Lamborg, C. H., Boyd, P. W., Lam, P. J., Trull, T. W., Bidigare, R. R., et al. (2007). Revisiting carbon flux through the ocean's twilight zone. *Science* 316, 567–570. doi:10.1126/science.1137959

Butman, C. A. (1986). Larval settlement of soft-sediment invertebrates: some predictions based on an analysis of near-bottom velocity profiles. *Elsevier Oceanogr. Ser.* 42, 487–513. doi:10.1016/S0422-9894(08)71061-4

Chaabane, S., de Garidel-Thoron, T., Giraud, X., Schiebel, R., Beaugrand, G., Brummer, G. J., et al. (2023). The forcis database: A global census of planktonic foraminifera from ocean waters. *Sci. Data* 10, 1–16. doi:10.1038/s41597-023-02264-2

Chaudhuri, S., Juan, P., and Serra, L. (2021). Analysis of precise climate pattern of Maldives. A complex island structure. *Regional Stud. Mar. Sci.* 44, 101789. doi:10.1016/j.rsma.2021.101789

Chowdhury, K. R., Haque, M. M., Nasreen, N., and Hasan, M. R. (2003). Distribution of planktonic foraminifera in the northern Bay of Bengal. *Sediment. Geol.* 155, 393–405. doi:10.1016/S0037-0738(02)00189-6

Clemens, S., Prell, W., Murray, D., Shimmield, G., and Weedon, G. (1991). Forcing mechanisms of the Indian Ocean monsoon. *Nature* 353, 720–725. doi:10.1038/353720a0

Conan, S. M. H., and Brummer, G. J. A. (2000). Fluxes of planktic foraminifera in response to monsoonal upwelling on the Somalia Basin margin. *Deep-Sea Res. II* 47, 2207–2227. doi:10.1016/S0967-0645(00)00022-9

Copernicus (2020). *Global Ocean physics Reanalysis*. Göttingen, Germany: Copernicus. doi:10.48670/moi-00021

Curry, W. B., Ostermann, D. R., Guptha, M. V. S., and Ittekkot, V. (1992). "Foraminifera production and monsoonal upwelling in the Arabian Sea: evidence from sediment traps," in *Upwelling systems: Evolution since the early miocene*. Editors C. P. Summerhayes, W. L. Prell, and K. C. Emeis (London, UK: Geological Society), 64, 93–106. doi:10.1144/GSL.SP.1992.064.01.061

Duplessy, J. C., Bé, A. W. H., and Blanc, P. L. (1981). Oxygen and carbon isotopic composition and biogeographic distribution of planktonic foraminifera in the Indian Ocean. *Palaeogeogr. Palaeoclimatol. Palaeoecol.* 33, 9–46. doi:10.1016/0031-0182(81)90031-6

Emery, W. J. (2019). "Water types and water masses," in *Encyclopedia of ocean science*. Editors J. K. Cochran, H. J. Bokuniewicz, and P. L. Yager (Amsterdam, Netherlands: Elsevier), 169–179. doi:10.1016/B978-0-12-409548-9.04426-2

Gebco Compilation Group (2022). GEBCO 2022 grid. https://www.gebco.net/data_and_products/gridded_bathymetry_data/gebco_2022/.doi:10.5285/e0f0bb80-ab44-2739-e053-6c86abc0289c

Gischler, E., Storz, D., and Schmitt, D. (2013). Sizes, shapes, and patterns of coral reefs in the Maldives, Indian ocean: the influence of wind, storms, and precipitation on a major tropical carbonate platform. *Carbonate Evaporites* 29, 73–87. doi:10.1007/s13146-013-0176-z

Global Administrative Areas (2022). GADM database of global administrative areas, version 4.1. URL: www.gadm.org.

Guptha, M. V. S., Curry, W. B., Ittekkot, V., and Muralinath, A. S. (1997). Seasonal variation in the flux of planktonic foraminifera: sediment trap results from the Bay of Bengal, Northern Indian Ocean. *J. Foraminifer. Res.* 27 (1), 5–19. doi:10.2113/gsjfr.27.1.5

Hemleben, C., Spindler, M., and Anderson, O. R. (1989). *Modern planktonic foraminifera*. Berlin, Germany: Springer-Verlag.

Kench, P. S., and Brander, R. W. (2006). Response of reef island shorelines to seasonal climate oscillations: south Maalhosmadulu atoll, Maldives. *J. Geophys. Res.* 111, F01001. doi:10.1029/2005JF000323

Kottek, J., Grieser, J., Beck, C., Rudolf, B., and Rubel, F. (2006). World Map of the Köppen-Geiger climate classification updated. *Meteorol. Z.* 15, 259–263. doi:10.1127/0941-2948/2006/0130

Loeblich, A. R., and Tappan, H. (1994). Foraminifera of the sahul shelf and Timor Sea. *Cushman Found. Foraminifer. Res.* 31.

Lüdmann, T., Betzler, C., Eberli, G. P., Reolid, J., Reijmer, J. J. G., Sloss, C. R., et al. (2018). Carbonate delta drift: A new sediment drift type. *Mar. Geol.* 401 (5), 98–111. doi:10.1016/j.margeo.2018.04.011

Lüdmann, T., Betzler, C., Lindhorst, S., Lahajnar, N., and Hübscher, C. (2022b). Submarine landsliding in carbonate ooze along low-angle slopes (Inner Sea, Maldives). *Mar. Petroleum Geol.* 136, 105403. doi:10.1016/j.marpetgeo.2021.105403

Lüdmann, T., Betzler, C., and Lindhorst, S. (2022a). The Maldives, a key location of carbonate drifts. *Mar. Geol.* 450. doi:10.1016/j.margeo.2022.106838

Lüdmann, T., Kalvelage, C., Betzler, C., Fürstenau, J., and Hübscher, C. (2013). The Maldives, a giant isolated carbonate platform dominated by bottom currents. *Mar. Petroleum Geol.* 43, 326–340. doi:10.1016/j.marpetgeo.2013.01.004

National Aeronautics and Space Administration (2022). Giovanni. Earth data. https://giovanni.gsfc.nasa.gov.

National Oceanic and Atmospheric Administration (2023). Dataset. Climate data library. https://iridl.ldeo.columbia.edu/SOURCES/.NOAA/. NCEP - NCAR/.CDAS-/.DAILY/.Diagnostic/.above_ground/.

National Oceanic and Atmospheric Administration (2015). National Centers for environmental prediction. Climate data library. http://iridl.ldeo.Columbia.edu/SOURCES/. NOAA/.NCEP/.EMC.CMB/.GLOBAL/.Reyn_SmithOIv2/.weekly/.

National Oceanic and Atmospheric Administration (2022). Ocean surface current analyses real-time. http://www.oscar.noaa.gov/datadisplay/oscar_datadownload.php.

Owen, A., Kruijsen, J., Turner, N., and Wright, K. (2011). *Marine energy in the Maldives. Prefeasibility Report on scottish Support for Maldives marine energy implementation, main report. Centre for understanding sustainable practice (CUSP)*. Schoolhill, Scotland: Robert Gordon University, 29.

Parker, J. H., and Gischler, E. (2011). Modern foraminiferal distribution and diversity in two atolls from the Maldives, Indian Ocean. *Mar. Micropaleontol.* 78, 30–49. doi:10.1016/j.marmicro.2010.09.007

Preu, C., and Engelbrecht, C. (1991). "Patterns and processes shaping the present morphodynamics of coral reef islands. Case study from the North-Male atoll, Maldives (Indian Ocean)," in *From the North sea to the Indian ocean*. Editors H. Brückner and U. Radtke (Stuttgart: Franz Steiner), 209–220.

Ramaswamy, V., and Gaye, B. (2006). Regional variations in the fluxes of foraminifera carbonate, coccolithophorid carbonate and biogenic opal in the northern Indian Ocean. *Deep-Sea Res. I* 53, 271–293. doi:10.1016/j.dsr.2005.11.003

Ran, L., Chen, J., Wiesner, M. G., Ling, Z., Lahajnar, N., Yang, Z., et al. (2015). Variability in the abundance and species composition of diatoms in sinking particles in the northern south China sea: results from time-series moored sediment traps. *Deep-Sea Res. II* 122, 15–24. doi:10.1016/j.dsr2.2015.07.004

Raza, T., and Ahmad, S. (2013). Surface and deep water variations in the northeast Indian Ocean during 34-6 ka BP: evidence from carbon and oxygen isotopes of fossil foraminifera. *Quat. Int.* 298, 37–44. doi:10.1016/j.quaint.2012.05.005

Reolid, J., Reolid, M., Betzler, C., Lindhorst, S., Wiesner, M. G., and Lahajnar, N. (2017). Upper pleistocene cold-water corals from the Inner Sea of the Maldives: taphonomy and environment. *Facies* 63, 8. doi:10.1007/s10347-016-0491-7

Saito, T., Thompson, P. R., and Breger, D. (1981). *Systemic undex of recent and pleistocene planktonic foraminifera*. Tokyo, China: University Tokyo Press.

Sasamal, S. K. (2006). Island mass effect around the Maldives during the winter months of 2003 and 2004. *Int. J. Remote Sens.* 27 (20), 5087–5093. doi:10.1080/01431160500177562

Sasamal, S. K. (2007). Island wake circulation off Maldives during boreal winter, as visualised with MODIS derived chlorophyll-adata and other satellite measurements. *Int. J. Remote Sens.* 28 (5), 891–903. doi:10.1080/01431160600858459

Sautter, L. R., and Thunell, R. C. (1991). Planktonic foraminiferal response to upwelling and seasonal hydrographic conditions: sediment trap results from San Pedro Basin, Southern California Bight. *J. Foraminifer. Res.* 21 (4), 347–363. doi:10.2113/gsjfr.21.4.347

Schiebel, R., and Hemleben, C. (2001). Protozoa, Planktonic foraminifera. *Encycl. Ocean Sci.* 4, 606–612. doi:10.1016/B978-012374473-9.00192-2

Schott, F. A., and McCreary, J. P., Jr. (2001). The monsoon circulation of the Indian Ocean. *Prog. Oceanogr.* 51, 1–123. doi:10.1016/S0079-6611(01)00083-0

Schulz, H., Von Rad, U., and Ittekkot, V. (2002). "Planktic foraminifera, particle flux and oceanic productivity off Pakistan, NE Arabian Sea: modern analogues and application to the palaeoclimatic record," in *The tectonic and climatic evolution of the Arabian Sea region*. Editors P. D. Clift, D. Kroon, C. Gaedicke, and J. Craig (London, UK: The Geological Society of London), 499–516.

Shen, W., Qiao, S., Sun, R., He, Z., Wu, B., Jin, L., et al. (2023). Distribution pattern of planktonic and benthic foraminifera in surface sediments near the equatorial Western Indian Ocean and its indications of paleo-environment and productivity. *J. Asian Earth Sci.* 250, 105635. doi:10.1016/j.jseaes.2023.105635

Storz, D., and Gischler, E. (2011). Coral extension rates in the NW Indian ocean I: reconstruction of 20th century SST variability and monsoon current strength. *Geo-Marine Lett.* 31, 141–154. doi:10.1007/s00367-010-0221-z

Storz, D., Gischler, E., Parker, J., and Klostermann, L. (2014). Changes in diversity and assemblages of foraminifera through the Holocene in an atoll from the Maldives, Indian Ocean. *Mar. Micropaleontol.* 106, 40–54. doi:10.1016/j.marmicro.2013.12.001

Tang, L. G., Su, X., Yang, Y. P., and Xiang, R. (2021). Sedimentary response to sea level and climate changes in the inner sea of Maldives carbonate platform over the past 30 kyr. *Paleoworld* 30 (3), 573–582. doi:10.1016/j.palwor.2020.09.003

Tantawy, A. A. A., Keller, G., and Pardo, A. (2009). Late Maastrichtian volcanism in the Indian Ocean: effects on calcareous nannofossils and planktic foraminifera. *Palaeogeogr. Palaeoclimatol. Palaeoecol.* 284, 63–87. doi:10.1016/j.palaeo.2009.08.025

Thunell, R. C., and Reynolds, L. A. (1984). Sedimentation of planktonic foraminifera: seasonal changes in species flux in the Panama Basin. *Micropaleontology* 30 (3), 243–262. doi:10.2307/1485688

Unger, D., Ittekkot, V., Schäfer, P., Tiemann, J., and Reschke, S. (2003). Seasonality and interannual variability of particle fluxes to the deep Bay of bengal: influence of riverine input and oceanographic processes. *Deep-Sea Res. II* 50, 897–923. doi:10.1016/S0967-0645(02)00612-4

Wang, D., Ding, X., and Bassinot, F. (2021). Observations of contrasted glacial-interglacial dissolution of foraminifera above the lysocline in the Bay of Bengal, northeastern Indian Ocean. *Acta Oceanol. Sin.* 40 (1), 155–161. doi:10.1007/s13131-021-1821-3

Xu, X., Yamasaki, M., Oda, M., and Honda, M. C. (2005). Comparison of seasonal flux variations of planktonic foraminifera in sediment traps on both sides of the Ryukyu Islands, Japan. *Mar. Micropaleontol.* 58 (1), 45–55. doi:10.1016/j.marmicro.2005.09.002

Yamasaki, M., and Oda, M. (2003). Sedimentation of planktonic foraminifera in the East China Sea: evidence from a sediment trap experiment. *Mar. Micropaleontol.* 49, 3–20. doi:10.1016/s0377-8398(03)00024-0

Young, J. R., Wade, B. S., and Huber, B. T. (2017). Pforams@mikrotax website. URL: http://www.mikrotax.org/pforams.